

# NN SCATTERING: CHIRAL PREDICTIONS FOR ASYMPTOTIC OBSERVABLES

J-L. Ballot<sup>1\*</sup>

*Division de Physique Théorique, Institut de Physique Nucléaire<sup>2†</sup>  
F-91406, Orsay CEDEX, France*

M.R. Robilotta<sup>3‡</sup>

*FINPE, Instituto de Física, Universidade de São Paulo  
C.P. 66318, 05389-970, São Paulo, SP, Brasil*

C.A. da Rocha<sup>4§</sup>

*Department of Physics, University of Washington  
Box 351560, Seattle, Washington 98195-1560, U.S.A.  
(March, 1997)*

## Abstract

We assume that the nuclear potential for distances larger than 2.5 fm is given just by the exchanges of one and two pions and, for the latter, we adopt a model based on chiral symmetry and subthreshold pion-nucleon amplitudes, which contains no free parameters. The predictions produced by this model for nucleon-nucleon observables are calculated and shown to agree well with both experiment and those due to phenomenological potentials.

PACS number(s): 21.30.+y, 13.75.Cs, 24.80.Dc, 25.80.Dj

Typeset using REVTeX

---

<sup>1\*</sup>Electronic address: ballot@ipno.in2p3.fr

<sup>2†</sup>Unité de Recherche des Universités Paris 6 et Paris 11 associé au CNRS.

<sup>3‡</sup>Electronic address: robilotta@if.usp.br

<sup>4§</sup>Present address: Instituto de Física Teórica (IFT), Universidade Estadual Paulista (UNESP) - R. Pamplona, 145 - 01405-900 - São Paulo, SP, Brazil. Electronic address: carocha@ift.unesp.br

## I. INTRODUCTION

In the last two decades several semiphenomenological potentials were proposed [1–5] which can describe rather well NN scattering data below the pion production threshold. All these models have a common feature, namely that the interaction at large distances is ascribed to the one-pion exchange potential (OPEP). On the other hand, they differ significantly at intermediate and short distances, a fact that becomes evident when one inspects the profile functions produced for the various components of the force. In each case, the reproduction of experimental data is achieved by means of a different balance between effects due to long and short distances. The fact that these potentials are successful means that somehow they are able to incorporate the relevant average dynamics.

At present, none of the existing semiphenomenological potentials include explicitly the dynamics associated with chiral symmetry, which constitutes the main conceptual framework for the study of strong interactions at energies which are small compared to the QCD scale. In this regime, non-perturbative effects are dominant and one is not able to do calculations using QCD directly. The usual strategy for overcoming this problem consists in working with an effective theory, constructed in such a way as to include as much as possible the main features of the basic theory. The masses of the quarks  $u$  and  $d$  are very small and hence their interactions with gluons are approximately invariant under the group  $SU(2) \times SU(2)$ . Therefore, one requires the effective theory at the hadron level posses the same basic symmetry, broken by just the pion mass.

In the last five years several authors have tackled the problem of NN interactions in the light of chiral symmetry and, so far, only processes associated with the two-pion exchange potential (TPEP) were systematically studied [6–15]. Chiral symmetry is very relevant to this component of the force because it controls the behaviour of the intermediate  $\pi N$  amplitude, that is the main building block of the interaction. The first works of this series were restricted to systems containing just pions and nucleons and considered basically the first five processes given in Fig.1 (A) [6–10,12]. These processes constitute an autonomous chiral family, incorporate correctly the well known cancellations of the intermediate  $\pi N$  amplitude [16,17] but correspond to an intermediate amplitude which is too simple for reproducing  $\pi N$  experimental data [18].

The extension of this minimal model so as to include other degrees of freedom was considered by Ordóñez, Ray and van Kolck [11,14] and by ourselves [13,15]. In the former case, a very general effective Lagrangian was used, which included explicitly the interactions of pions, nucleons and deltas and contained some free parameters representing other interactions. In principle, these parameters could be obtained from other physical processes, but these authors chose to adjust them to NN scattering data. Using a non-relativistic cut-off of the order of the rho mass, they could achieve a qualitative description of all NN observables.

In our approach, the intermediate  $\pi N$  amplitude involved the interactions of pions and nucleons, supplemented by empirical information in the form of the Höhler, Jacob and Strauss (HJS) coefficients [19]. In general, the physical amplitude for the process  $\pi^\alpha(k)N(p) \rightarrow$

$\pi^\beta(k')N(p')$  may be described by two independent variables,  $\nu = \frac{1}{4m}(p + p') \cdot (k + k')$  and  $t = (k - k')^2$ . In order to obtain the HJS coefficients, one subtracts the nucleon pole from the empirical  $\pi N$  amplitude and uses dispersion relations to continue analytically the remainder (R) to an unphysical region around the point  $\nu = 0, t = 0$ . The HJS coefficients are then obtained by expanding this remainder in a power series in  $\nu$  and  $t$ . The use of the subthreshold coefficients is particularly suited to the calculation of the TPEP at large distances, since this part of the potential is determined by the intermediate  $\pi N$  amplitude in the very neighbourhood of the point  $\nu = 0, t = 0$ . Thus, in this aspect, our approach is very different from that of Ordóñez, Ray, and van Kolck.

In our calculation, the TPEP was derived from the ten diagrams depicted in Fig.1, representing both interactions involving only nucleons (A) and other degrees of freedom (B). The main features of the asymptotic TPEP were extensively discussed in [15] and here we just recall some of the conclusions of that paper. One of them is that the scalar-isoscalar component of the TPEP at large distances is attractive and therefore qualitatively coherent with a well known feature of the nuclear force. As far as dynamics is concerned, we have shown that chiral symmetry is responsible for large cancellations in the pure nucleon sector (Fig.1, A) [16,17] and eventually the contributions from this sector turn out to be much smaller than those arising from other degrees of freedom. The main contribution to the intermediate attraction is due to processes containing nucleons in one leg and the remainder degrees of freedom in the other.

The fact that our calculation of the TPEP did not contain free parameters means that it yields predictions for NN observables, whose study is the main goal of the present work. We assume that, for distances larger than 2.5 fm, the NN interaction is given by just the OPEP and the TPEP calculated in ref. [15] and try to determine the values of the angular momentum and the energy regions for which observables can be ascribed to these components only. Our presentation is divided as follows: in Sec.II we discuss our method of work and in Sec.III we give our results and conclusions.

## II. DYNAMICS

In general, it is not easy to isolate unambiguously the observables associated with a particular region of a given potential. Nevertheless, in many cases, the centrifugal barrier can suppress a significant part of the short range interaction and one is left only with contributions from the tail of the force. For instance, in a study of the influence of the OPEP over NN observables, we have obtained, for most waves with  $\ell > 2$ , purely pionic phase shifts and mixing parameters, which did not depend on the short range features of the interaction [20]. In the case of the OPEP, this kind of result is possible because the potential is not too strong.

In the present problem, even if one is willing to consider the influence of the TPEP only for separations larger than 2.5 fm, where the results of Ref. [15] are mathematically reliable, one needs to use expressions which are valid for all distances. As it is important have close

control of the regions of the potential that contribute to the observables, we employ the so called variable phase method. It is fully equivalent to the Schrödinger equation and provides a clear spatial picture of the way phase shifts and mixing parameters are structured. For the sake of completeness, we summarize here the main equations used in our calculation. In the case of uncoupled channels, the wave function  $u_J(r)$  with angular momentum  $J$  is written as [21]

$$u_J(r) = c_J(k, r) \hat{j}_J(kr) - s_J(k, r) \hat{n}_J(kr) , \quad (1)$$

where  $\hat{j}_J$  and  $\hat{n}_J$  are the usual Bessel and Neumann functions multiplied by  $kr$ . The functions  $c_J$  and  $s_J$ , for a potential  $V_J(r)$ , are given by

$$c_J(k, r) = 1 - \frac{m}{k} \int_0^r d\rho V_J(\rho) \hat{j}_J(k\rho) u_J(\rho) , \quad (2)$$

$$s_J(k, r) = -\frac{m}{k} \int_0^r d\rho V_J(\rho) \hat{n}_J(k\rho) u_J(\rho) . \quad (3)$$

The variable phase  $D_J(k, r)$  is defined as

$$D_J = \tan^{-1}\left(\frac{s_J}{c_J}\right) \quad (4)$$

and, by construction, it vanishes at the origin and yields the observable phase shift  $\delta_J$  when  $r$  tends to infinity. Differentiating (2) and (3), using (1), and manipulating the result, one obtains the differential equation

$$D'_J = -\frac{m}{k} V_J P_J^2(D_J) , \quad (5)$$

where  $D'_J = \frac{dD_J}{dr}$  and the structure function  $P_J$  is given by

$$P_J = \hat{j}_J \cos(D_J) - \hat{n}_J \sin(D_J) . \quad (6)$$

In the case of coupled channels, one has two phases,  $D_{Jm}$  and  $D_{Jp}$ , with  $m = L - 1$  and  $p = L + 1$ , and a mixing parameter  $E_J$ , that depend on  $r$  and become the observables  $\delta_{Jm}$ ,  $\delta_{Jp}$  and  $\epsilon_J$  when  $r$  tends to infinity. Denoting the diagonal and tensor components of the potential by  $W_{JL}$  and  $T_J$ , one has the following coupled differential equations [22]

$$\begin{aligned} D'_{Jm} = & -\frac{m}{k \cos(2E_J)} \left\{ W_{Jm} \left[ \cos^4(E_J) P_m^2 - \sin^4(E_J) Q_m^2 \right] \right. \\ & - W_{Jp} \sin^2(E_J) \cos^2(E_J) (P_p^2 - Q_p^2) \\ & \left. - 2 T_J \sin(E_J) \cos(E_J) \left[ \cos^2(E_J) P_m Q_p - \sin^2(E_J) P_p Q_m \right] \right\} , \end{aligned} \quad (7)$$

$$E'_{Jm} = -\frac{m}{k} \left\{ T_J \left[ \cos^2(E_J) P_m P_p + \sin^2(E_J) Q_m Q_p \right] - W_{Jm} \sin(E_J) \cos(E_J) P_m Q_m - W_{Jp} \sin(E_J) \cos(E_J) P_p Q_p \right\} . \quad (8)$$

In these expressions the structure functions  $P_L$  and  $Q_L$  are defined as

$$P_L = \hat{j}_L \cos(D_{JL}) - \hat{n}_L \sin(D_{JL}) , \quad (9)$$

$$Q_L = \hat{j}_L \sin(D_{JL}) + \hat{n}_L \cos(D_{JL}) . \quad (10)$$

The equation for  $D_{Jp}$  is obtained by exchanging the labels  $m$  and  $p$  in (7).

As far as the interaction is concerned, we consider just the OPEP ( $V_\pi$ ) and the TPEP, which are assumed to represent the full potential for distances greater than 2.5 fm. As pointed out in the introduction, the TPEP is determined by two kinds of contributions, one generated in the pure pion-nucleon sector ( $V_N$ ) and the other associated with the remainder degrees of freedom ( $V_R$ ). The direct inspection of these potentials indicates that the former is comparable to the OPEP, whereas the latter is rather strong for  $r > 2.0$  fm. In order to calculate the observables, one needs to regularize the various potentials at short distances. In the case of OPEP, the regularization is achieved by cutting it at a radius  $r_\pi$  and replacing the inner part by the constant value  $V_\pi(r_\pi)$ . As  $V_N$  is comparable to the OPEP, we adopt the same regularization procedure for it, with a radius  $r_N$ .

The regularization of  $V_R$  is more problematic. For distances around 1.0 fm, the value of the central component of the potential is about  $-25$  GeV. On the other hand, in Ref. [15] we have argued that the asymptotic TPEP is mathematically reliable only for distances larger than 2.5 fm, indicating that the odd behaviour of the TPEP at short distances is unphysical and associated with the use of equations outside their domain of validity. Inspecting the equations used in that work, it is easy to relate this behaviour to the HJS coefficients involving high powers of  $\nu$  and  $t$  in the intermediate  $\pi N$  amplitude. On the other hand, restricting ourselves to the first two leading contributions, due to the coefficients of the terms  $\nu^0 t^0$  and  $\nu^0 t^1$ , we keep most of the asymptotic potential and get values around  $-150$  MeV in the neighbourhood of 1.0 fm, which are still large, but much more reasonable. Therefore we base the present study on this leading potential, which is regularized by means of a step function  $\theta(r_R)$ .

In this calculation one can rely only on those results which are independent of the radii used in the regularization procedure. In order to control this independence, we adopt  $r_N = r_\pi$ , vary  $r_\pi$  in the interval  $0.8 - 1.0$  fm and discard the cases where the contribution of  $V_\pi + V_N$  to the observables varies more than 1.0%. Concerning  $V_R$ , the preceding discussion suggests that one should be interest in effects due to the region  $r > 2.5$  fm and hence we consider values of  $r_R$  between 1.5 fm and 2.5 fm and study the effect of this variation over the observables. This produces an indication of both the stability of the results and the

importance of the inner part of the potential. When the variation of the results is less than 5%, we take them as predictions of the potential. For larger deviations, we consider them as estimates.

### III. RESULTS AND CONCLUSIONS

We have calculated the predictions for NN observables produced by a chiral potential [15] involving only the exchanges of one and two pions, assumed to represent the full interaction for distances larger than 2.5 fm. Since we are interested only in the cases where the centrifugal barrier cuts naturally the inner parts of the force, we used the variable phase method to control this aspect of the problem. One may acquire a feeling for this method by looking at Fig. 2, where we display the variable phases for the wave  $^1G_4$ , divided by their asymptotic values, for three different energies. It is possible to see that, as expected, higher energies probe more the interior of the potential. It is also interesting to note that the variable phase method allows one to make quantitative statements such as, for instance, the radius for which the phase attains a given percentage of its final value.

In the case of uncoupled waves, the interplay between the centrifugal barrier and the regularization of the background is rather intuitive, but this is not the case of coupled systems. In order to clarify this point, we show in Fig. 3 the variable phases for the  $^3D_3 - ^3G_3$  system for  $E = 200$  MeV, due just to the background and regularized at either at 0.7 fm or 1.0 fm. One sees that the  $^3D_3$  curves depend strongly on the cutoff, whereas those describing  $\epsilon_3$  and  $^3G_3$  are very stable and cannot be distinguished with the naked eye. The wave  $^3G_3$  is negligible for distances smaller than 2.0 fm due to the centrifugal barrier, meaning that the system is effectively uncoupled up to that distance. The construction of  $^3D_3$  extends up to 3.5 fm, where  $\epsilon_3$  is maximum, but the two other observables become asymptotic much later, around 5.0 fm. This indicates that, even for coupled waves, the various components get their contributions from different regions in space.

We found out that the observables associated with the following waves depend more than 1% on the cutoff used for the  $V_\pi + V_N$  background and hence are not suited for our study:  $^1S_0$ ,  $^3P_0$ ,  $^3P_2$ ,  $^3S_1$ ,  $\epsilon_1$ ,  $^3D_1$  and  $^3D_3$ .

In Figs. 4-7, we display our results for the phase shifts as a function of the laboratory energy. They include predictions from the OPEP cut at 1.0 fm, the sum of the OPEP and  $V_N$  cut at 1.0 fm and the total results produced by cutting the contribution of  $V_R$  at 1.5 fm ( $\chi(1.5)$ ) and 2.5 fm ( $\chi(2.5)$ ), and the experimental values are taken from SAID VZ40 solution [23]. For comparative purposes, we also include the predictions of the Argonne [4] phenomenological potential.

The dominant part of the chiral TPEP is associated with the exchange of a scalar-isoscalar system and hence its significance depends strongly on the NN channel considered. Therefore in the sequence we comment the main features of our results for the various subspaces of spin and isospin.

(**T=1,S=0**); Fig. 4: There are no results for the wave  $^1S_0$ , since it cannot be understood

as a TPEP superimposed to a pionic background. For the waves  $^1D_2$  and  $^1G_4$  one has predictions for energies up to 50 MeV and 300 MeV respectively. As expected, the TPEP increases the attraction due to the OPEP and our results are very close to the experimental values for the potential cut at 2.5 fm.

**( $T=1, S=1$ );** Figs. 5a,b,c,d: The waves  $^3P_0$  and  $^3P_2$  depend on the pion cutoff and were discarded. For the uncoupled waves  $^3P_1$ ,  $^3F_3$ , and  $^3H_5$  (Fig. 5a) we obtain predictions which extend up to 300 MeV for the last two of them. Results for the waves  $^3P_1$  and  $^3F_3$  are compatible with experiment, but this does not happen for the  $^3H_5$  wave. In the case of the coupled waves, that with lowest orbital angular momentum tend, as expected, to be much more influenced by the cutoff used for the OPEP than the other ones. We obtain predictions in all cases, but the mixing parameters are heavily dominated by the OPEP and yield very little information about the TPEP. For the waves  $^3F_2$  (Fig. 5b) and  $^3F_4$  (Fig. 5c), the differences with experimental values are small, whereas for the waves  $^3H_4$  (Fig. 5c) and  $^3H_6$  (Fig. 5d) they are important.

**( $T=0, S=0$ );** Fig. 6: Our calculation yields predictions for all the waves in this sector, namely  $^1P_1$ ,  $^1F_3$ , and  $^1H_5$ , generally quite close to the pure OPEP ones, reflecting the fact that our central potential in this channel is small. Results are also close to experiment.

**( $T=0, S=1$ );** Figs. 7a,b,c: The observables  $^3S_1$ ,  $\epsilon_1$ ,  $^3D_1$  and  $^3D_3$  depend on the pion cutoff and are not considered. In all cases, coupled and uncoupled, our results are dominated by the OPEP and close to experiment.

In order to assess the general trends of the various observables presented in Figs. 4-7, it is useful to recall that the relative strengthes of the central and tensor OPEP in the channels  $(T, S) = (1, 0), (1, 1), (0, 0)$ , and  $(0, 1)$  are respectively  $1 : \frac{1}{3} : 3 : 1$  and  $0 : \frac{1}{3} : 0 : 1$ . This means that one pion exchange is more important in the channels with  $T = 0$  and hence the good agreement between predictions and experimental results noted in Figs. 6 and 7 may be ascribed to OPEP physics.

As far as the channels with  $T = 1$  are concerned (Figs. 4 and 5), the tensor interaction makes the OPEP to be more important for triplet waves, in spite of its weaker central component. Therefore the role of the TPEP is more evident in the waves  $^1D_2$  and  $^1G_4$  (Fig. 4), where chiral predictions agree well with experiment. In the case of triplet waves (Figs. 5a,b,c,d), one also finds that the chiral potential is able to reproduce experimental data when  $\ell < 5$ , but this does not happen for  $H$  waves. The behavior of these waves are peculiar, since they have a high orbital angular momentum and hence should be close of being OPEP dominated. Indeed, our results show that predictions from the chiral potential for  $H$  waves are not far from the OPEP and also depend little on the cutting radius. Part of the discrepancies observed may be associated with the fact that we have used  $g^2/4\pi = 14.28$  for the  $\pi N$  coupling constant [19] whereas the SAID analysis is based on the value  $g^2/4\pi = 13.7$ . It is also worth pointing out that there is a 10% difference between the experimental  $pn$  and  $pp$  solutions and the discrepancies would be reduced if the latter were used. However, even if these factors were considered, the experimental data would still seem to suggest that the TPEP is repulsive for the waves  $^3H_4$  and  $^3H_6$ , something which is rather difficult to explain

theoretically.

A general conclusion that can be drawn from the present study concerns the details of the TPEP. As discussed in the introduction and represented in Fig. 1, it consists in a sum of terms, arising from both the pure pion nucleon sector and from interactions involving other degrees of freedom. Our results show that the former contributions are very small, indicating that the numerical significance of the TPEP is essentially due to the interplay between nucleon and other degrees of freedom.

In this work we tested the chiral TPEP derived in Ref. [15], which is based on subthreshold  $\pi N$  data and contains no free parameters. Our results have shown that it is rather consistent with experiment<sup>1</sup>.

#### IV. ACKNOWLEDGMENTS

M.R.R would like to thank the kind hospitality of the Division de Physique Theorique de l’Institut de Physique Nucleaire, Orsay, France, where this work was performed and FAPESP (Brazilian Agency), for financial support. The work of C.A. da Rocha, was supported by Grant No. 200154/95-8 from CNPq Brazilian agency. This work was partially supported by U.S. Department of Energy.

---

<sup>1</sup>Note added in revision: In a recent work, the predictions from a similar chiral potential were presented [24], which agree qualitatively with those produced here.



## REFERENCES

- [1] R. de Tourreil and D.W.L. Sprung, Nucl. Phys. A **201**, 193 (1973).
- [2] R. de Tourreil, B. Rouben, and D.W.L. Sprung, Nucl. Phys. A **242**, 445 (1975).
- [3] M. Lacombe, B. Loiseau, J-M Richard, and R. Vinh Mau, Phys. Rev. C **21**, 861 (1980).
- [4] R.B. Wiringa, R.A. Smith, and T.L. Ainsworth, Phys. Rev. C **29**, 1207 (1984).
- [5] R. Machleidt, K. Holinde, and C. Elster, Phys. Rep. **149**, 1 (1987).
- [6] C. Ordóñez and U. van Kolck, Phys. Lett. B **291**, 459 (1992).
- [7] L.S. Celenza, A. Pantziris, and C.M. Shakin, Phys. Rev. C **46**, 2213 (1992).
- [8] J.L. Friar and S.A. Coon, Phys. Rev. C **49**, 1272 (1994).
- [9] C.A. da Rocha and M.R. Robilotta, Phys. Rev. C **49**, 1818 (1994).
- [10] M.C. Birse, Phys. Rev. C **49**, 2212 (1994).
- [11] C. Ordóñez, L. Ray, and U. van Kolck, Phys. Rev. Lett. **72**, 1982, (1994).
- [12] C.A. da Rocha and M.R. Robilotta, Phys. Rev. C **52**, 531 (1995).
- [13] M.R. Robilotta, Nucl. Phys. A **595**, 171 (1995).
- [14] C. Ordóñez, L. Ray, and U. van Kolck, Phys. Rev. C **53**, 2086, (1996).
- [15] M.R. Robilotta and C.A. da Rocha, Nucl. Phys. A **615**, 391 (1997).
- [16] J-L. Ballot and M.R. Robilotta, Z. Phys. A **355**, 81 (1996).
- [17] J-L. Ballot, M.R. Robilotta, and C.A. da Rocha, Int. J. Mod. Phys. E **6**, 83 (1997).
- [18] G.Höhler, group I, vol.9, subvol.b, part 2 of Landölt-Börstein Numerical Data and Functional Relationships in Science and Technology, ed. H. Schopper, 1983.
- [19] G.Höhler, H.P.Jacob, and R.Strauss, Nucl. Phys. B **39**, 237 (1972).
- [20] J-L. Ballot and M.R. Robilotta, J. Phys. G **20**, 599 (1994).
- [21] F. Calogero, N. Cim. **27**, 261 (1963); *Variable Phase Approach for Potential Scattering* (New York: Academic 1967).
- [22] V.V. Babikov, Sov. Phys. Usp. **92**, 271 (1967).
- [23] R.A. Arndt, I.I. Strakovsky, and R.L.Workman, Phys. Rev. C **50**, 2731 (1994); internet WWW interactive results at [http : //clsaid.phys.vt.edu/ ~CAPS/](http://clsaid.phys.vt.edu/~CAPS/)
- [24] N. Kaiser, R. Brockmann, and W. Weise, preprint nucl-th/9706045.

# FIGURES

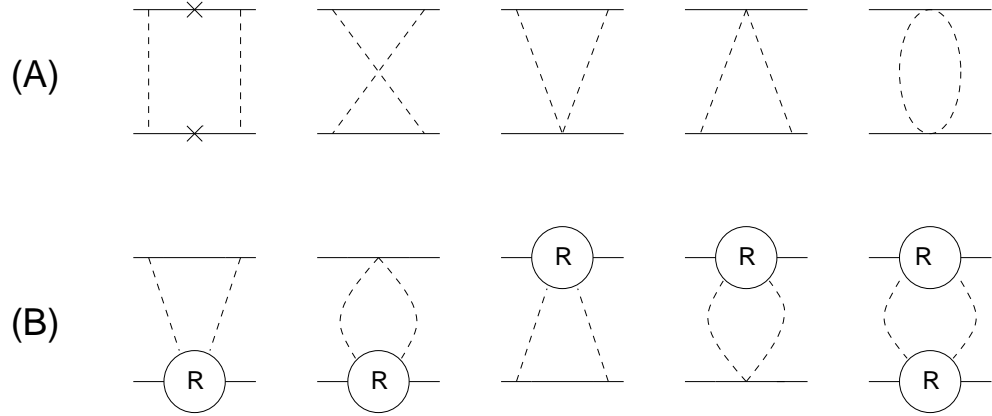


FIG. 1. Contributions to the two-pion exchange nucleon-nucleon potential from the pure pion-nucleon sector (A) and for processes involving other degrees of freedom (B). The crosses in the nucleon lines of the first diagram indicate that the iterated OPEP was subtracted.

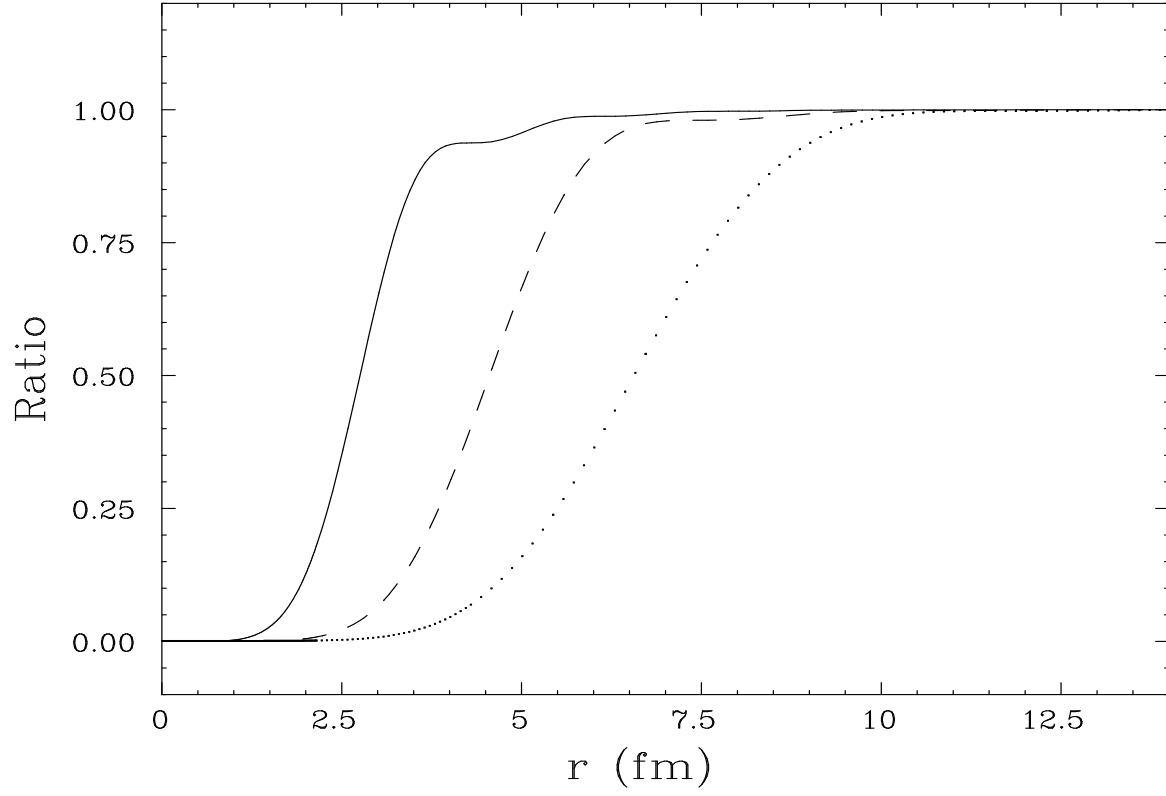


FIG. 2. Variable phases (normalized to 1) for the wave  $^1G_4$  at the energies  $E = 40$  MeV (dotted line),  $E = 100$  MeV (dashed line) and  $E = 300$  MeV (continuous line).

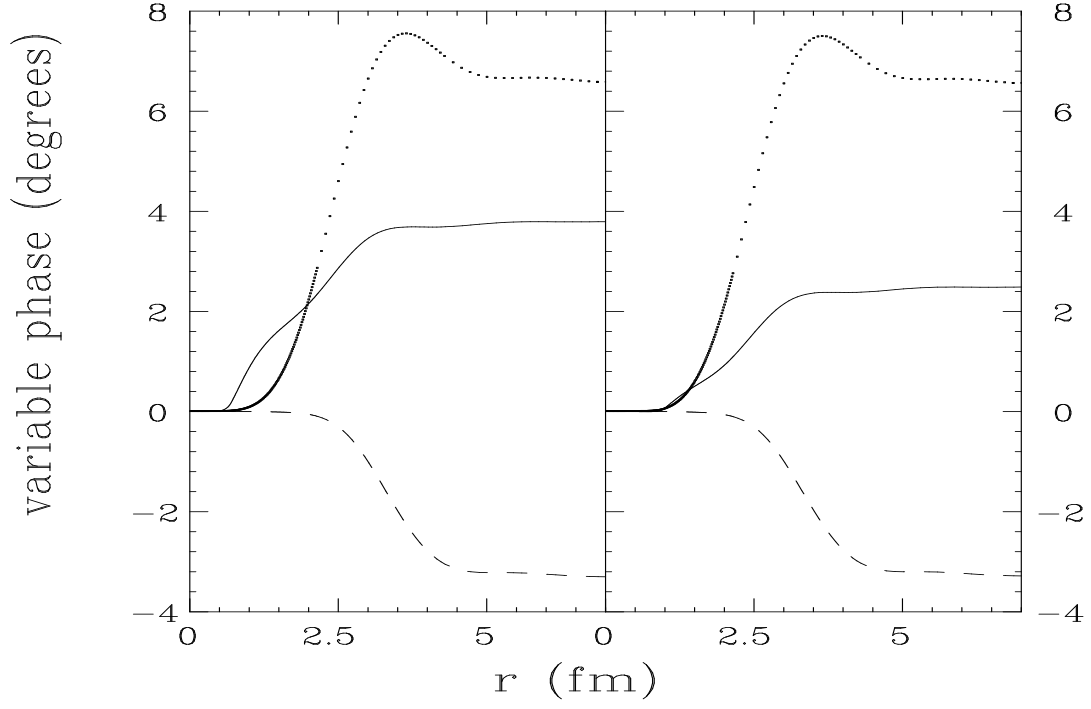


FIG. 3. Variable phases for the waves  ${}^3D_3$  (dotted line),  ${}^3G_3$  (dashed line) and the mixing parameter  $\epsilon_3$  (solid line) for background potentials cut at 0.7 fm (left) and 1.0 fm (right).

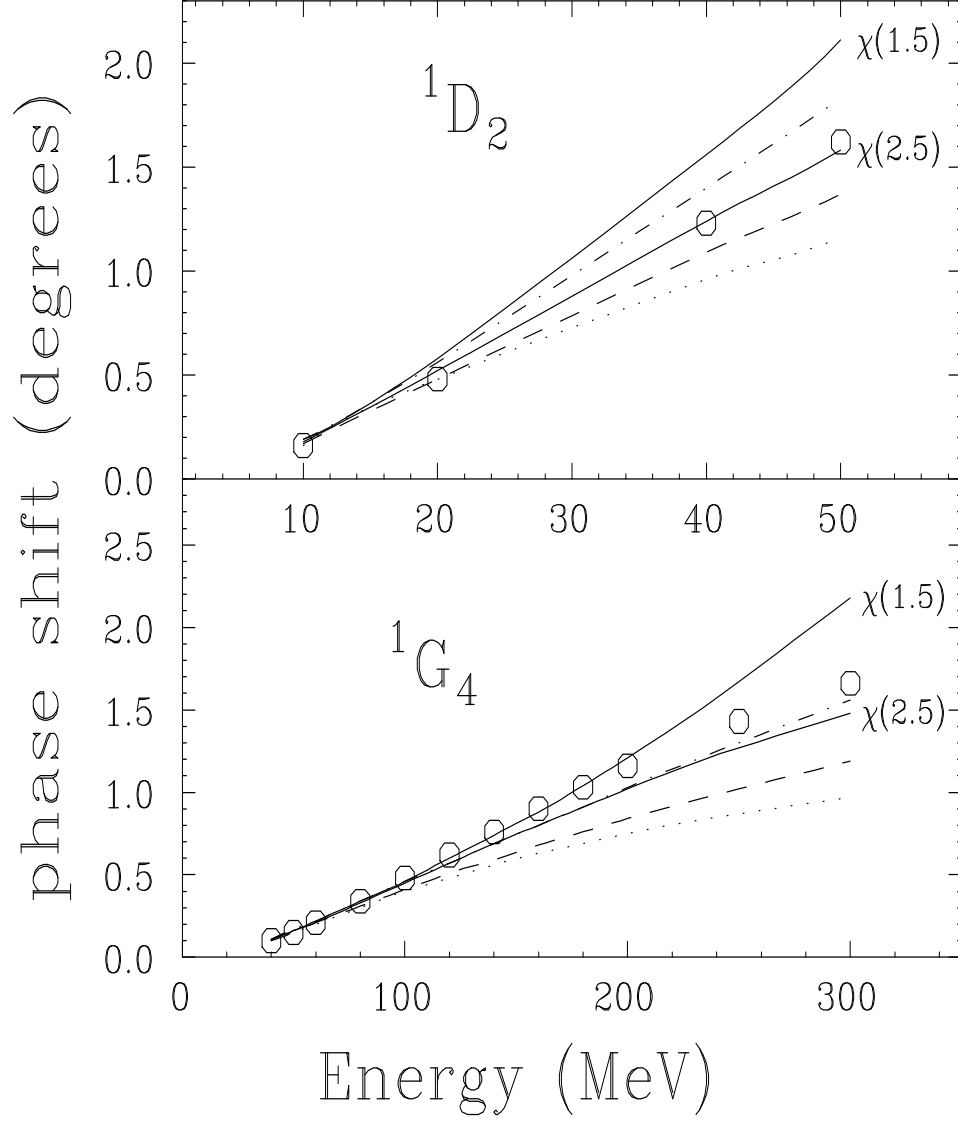


FIG. 4. Phase shifts for the channel ( $T = 1, S = 0$ ) due to the OPEP cut at 1.0 fm (dotted line), the sum of the OPEP and the pure pion-nucleon TPEP cut at 1.0 fm (dashed line) and the full chiral potential cut at 1.5 fm and 2.5 fm (continuous lines labeled  $\chi(1.5)$  and  $\chi(2.5)$ ). For comparative purposes, the predictions of the argonne v14 potential are also included (dashed-dotted line). The experimental points represent the  $pn$  solution of SAID [23].

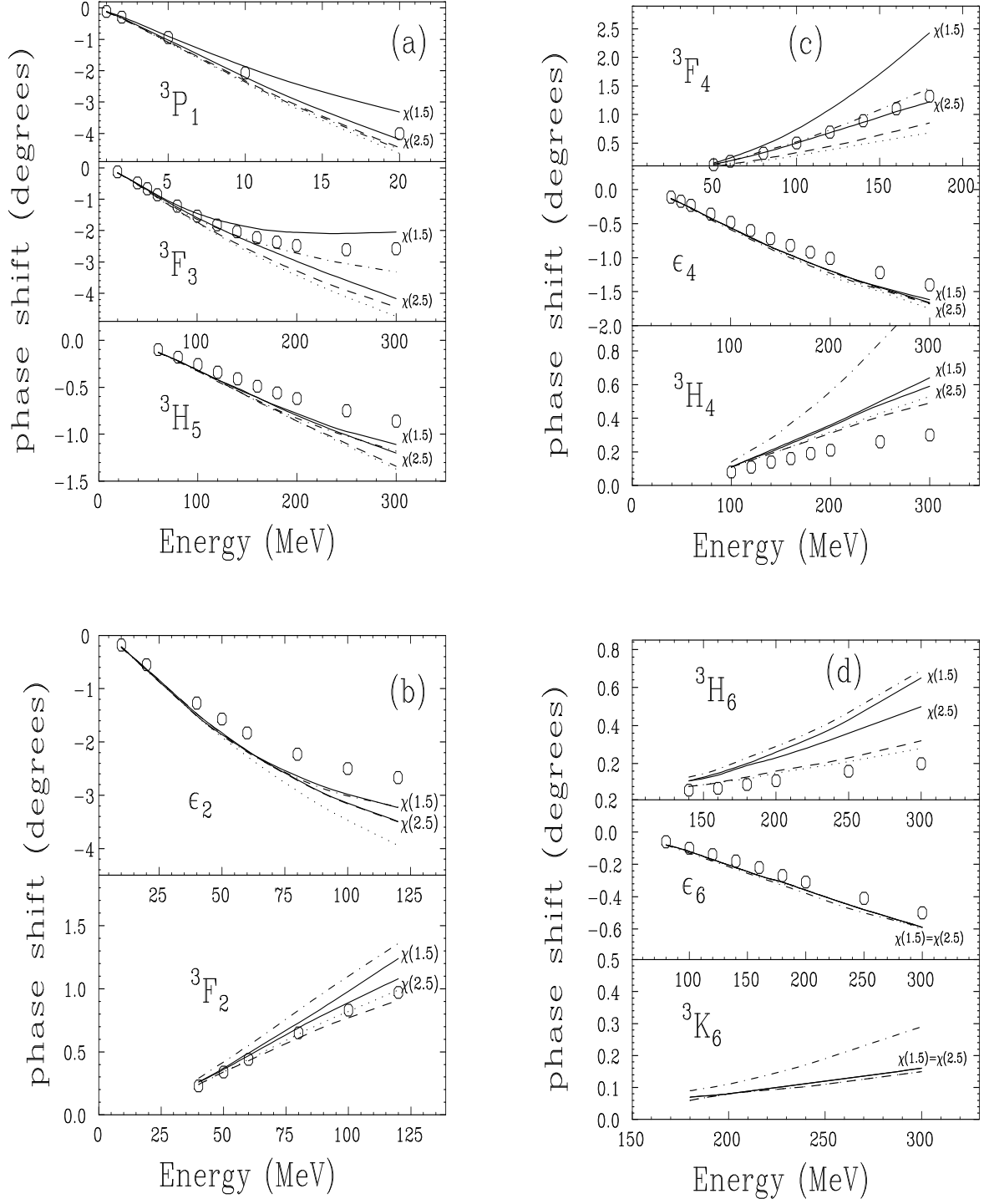


FIG. 5. Phase shifts for the channel  $(T = 1, S = 1)$ ; (a) uncoupled waves; (b)  $J = 2$  coupled channel; (c)  $J = 4$  coupled channel; (d)  $J = 6$  coupled channel. Conventions are given in Fig. 4.

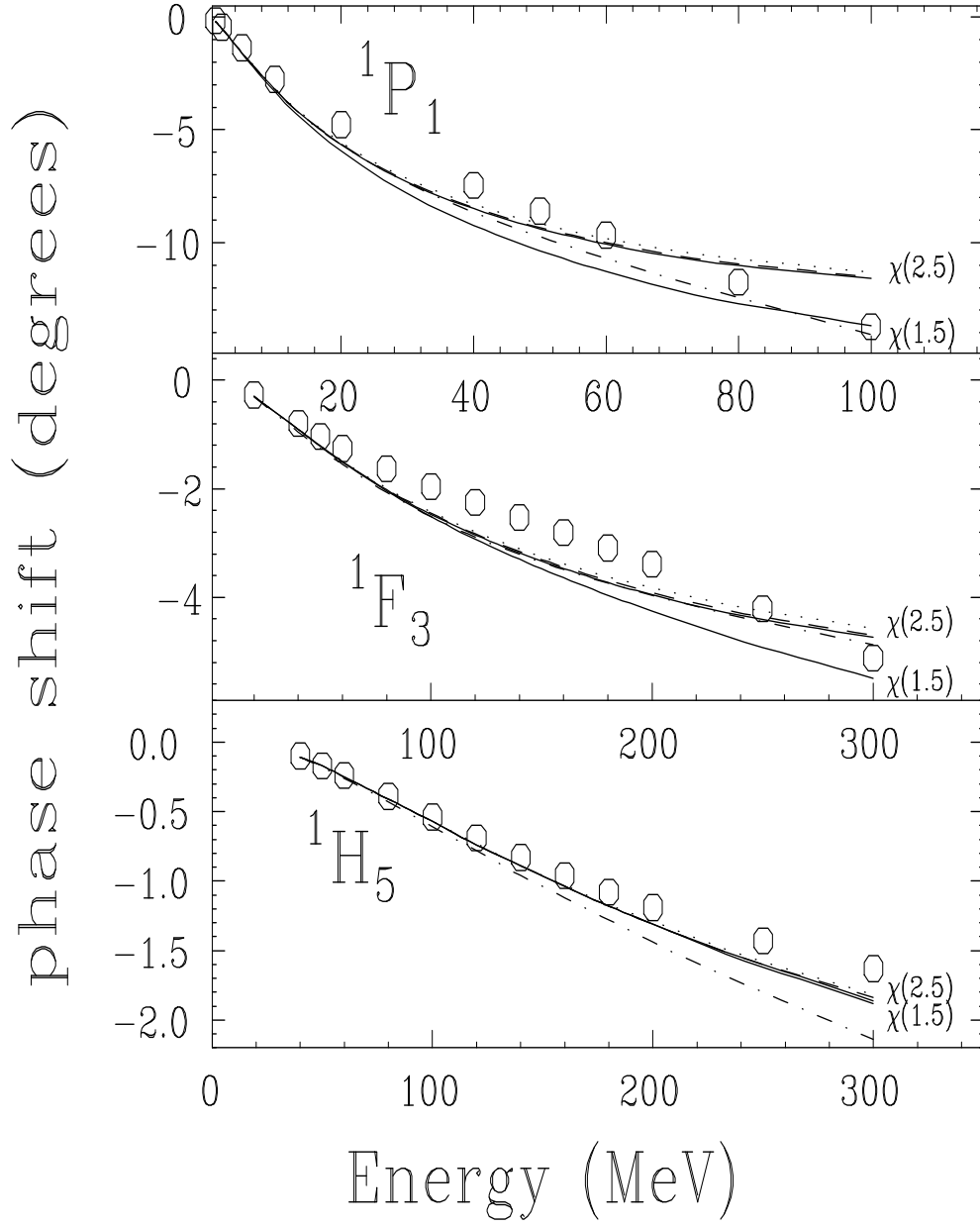


FIG. 6. Phase shifts for the channel ( $T = 0, S = 0$ ); conventions are given in Fig. 4.

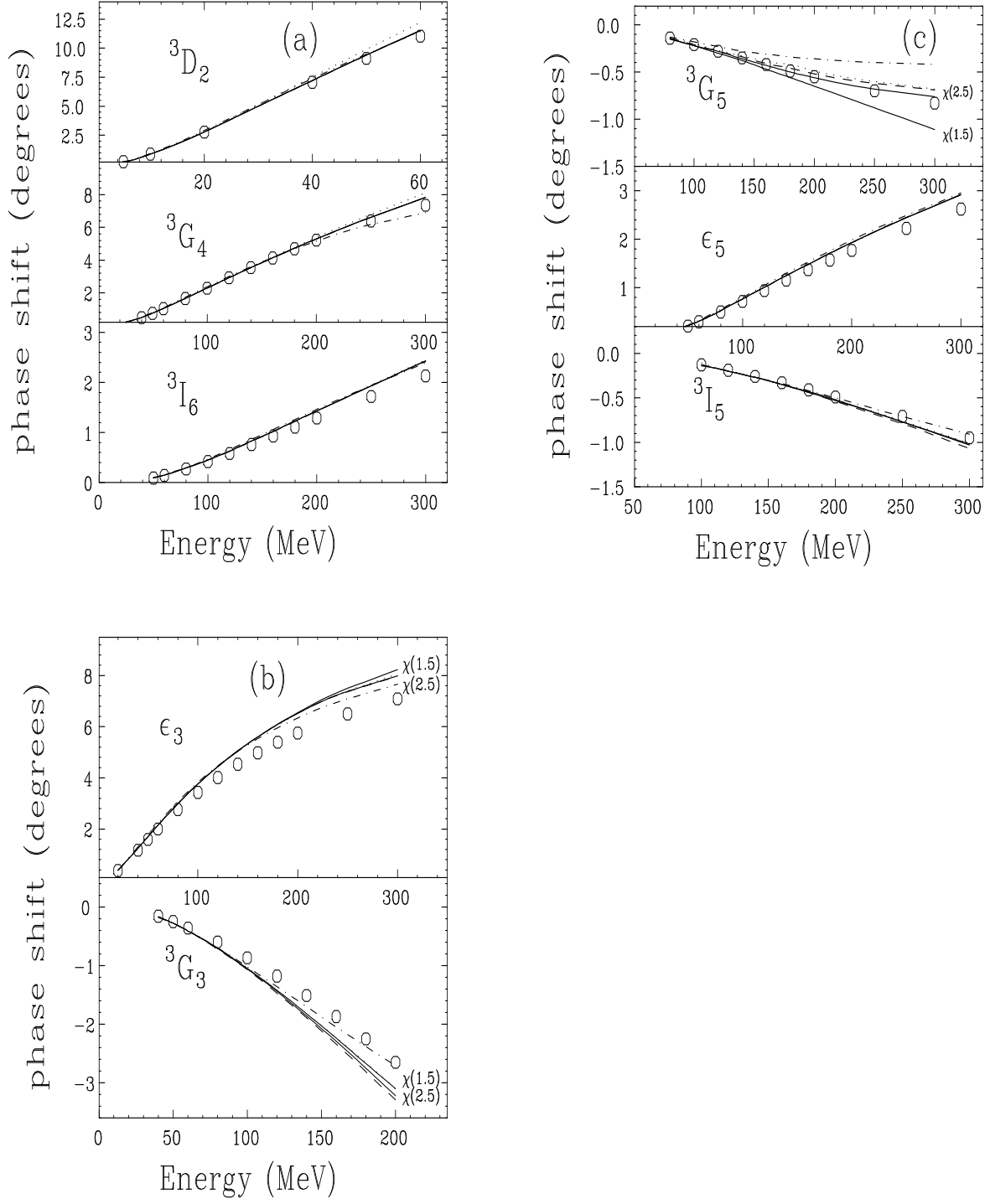


FIG. 7. Phase shifts for the channel  $(T = 1, S = 1)$ ; (a) uncoupled waves; (b)  $J = 3$  coupled channel; (c)  $J = 5$  coupled channel. Conventions are given in Fig. 4.